Post Stall Studies of Untwisted Varying Aspect Ratio Blades with NACA 44XX Series Airfoil Sections – Part II.

C. Ostowari (1) and D. Naik (2).
Aerospace Engineering Department, Texas A&M University, College Station, Texas 77843, U.S.A.
(1) Assistant Professor
(2) Graduate Research Assistant

ABSTRACT

In Part I of this paper results were presented from a wind tunnel investigation of untwisted, constant chord blades with an NACA 4415 series airfoil section and at angles of attack ranging from −10 to 110 degrees. Tests were conducted for aspect ratios of infinity, 12, 9 and 6, at Reynolds numbers of 0.25, 0.50 0.75 and 1.00 million.

Part II discusses results from a similar series of tests conducted on varying thickness blades of the NACA 44XX series airfoil family. The new thickness ratios studied were 18, 12 and 9 and comparisons are made with the results presented in Part I. The test conditions for the present series of experiments are identical to the conditions for which results were presented in Part I. However, there is no comparison for the effects of boundary layer tripping on blades with the present thickness ratios.

Both initial and secondary stall are presented. For each thickness ratio, the maximum lift coefficient decreases with increasing Reynolds Number. The maximum drag coefficient is found to occur near an angle of attack of 90 degress. The pitching moment has a relatively flat pre-stall characteristic and beyond stall the slope is negative. The lift and post-stall drag coefficients decrease with decreasing aspect ratio. Secondary stall becomes less pronounced as the aspect ratio is decreased. For angles of attack up to and just beyond primary stall, the lift coefficient decreases with decreasing thickness ratio. In the post-stall region, the maximum drag coefficient generally increases with decreasing thicknes ratio. These thickness ratio effects are true for all the aspect ratios that were studied. The post-stall aerodynamic characteristics are more strongly affected by changes in aspect ratio than by changes in Reynolds number and thickness ratio.

SYMBOLS

The force and moment data have been referred to the quarter-chord location on the airfoil. Dimensional quantities are given in SI units. Measurements were made in U.S. Customary Units. The symbols used herein are defined as follows:

AR	Aspect ratio (b^2/S)
b	Span
c	Airfoil reference chord
C_D	Drag coefficient = Drag/(q × S)
C_L	Lift coefficient = Lift/(q x S)
C_M	Pitching moment coefficient with respect to the 0.25 c location = Moment/(q × S × c); Positive cloclwise.
q	Dynamic pressure
RN	Reynolds number with respect to c
S	Reference area (surface area)
t	Maximum thickness of the airfoil section
α	Angle of attack

INTRODUCTION

This paper presents the post stall aerodynamic characteristics, lift, drag and pitching moment, of untwisted constant chord blades as a function of airfoil thickness, aspect ratio and Reynolds number. This data is helpful for the design of cost effective wind energy conversion devices (Ref. 1) This study of three dimensional, cambered blades used the NACA 44XX series of airfoil sections. All possible combinations of the thickness ratios 18, 15, 12 and 9; aspect ratios ∞, 12, 9 and 6; and Reynolds nimbers of 0.25, 0.50, 0.75 and 1.00 million, were studied over the angle of attack range of -10 to 110 degress. In some cases, i.e. combinations of low thickness ratio, high aspect ratio and high Reynolds number, it was necessary to somewhat restrict the deep stall angle of attack range to prevent blade failure. A cross-section view of the four different airfoil thicknesses is shown in Figure 1. This figure also shows the bonded laminates that were used in the construction.

In addition to the large angle of attack variation, a wind turbine blade is also exposed to a considerable amount of atmospheric dirt, bird droppings and insect hits, especially near the leading edge. One might expect a corresponding deterioration in the aerodynamic performance of the blade. This problem was addressed in Part I of this paper, wherein an "unclean" blade was simulated by the strategic placement of strips of chart tape on the surface of a blade with an NACA 4415 section, and is not treated here.

The model description, test facility, test conditions and testing procedure for the experiments are given in Part I. The results presented here have been carefully selected to give the reader a fair representation of the aerodynamic ramifications of operating in deep stall conditions. The full complement of data is available in Reference 2.

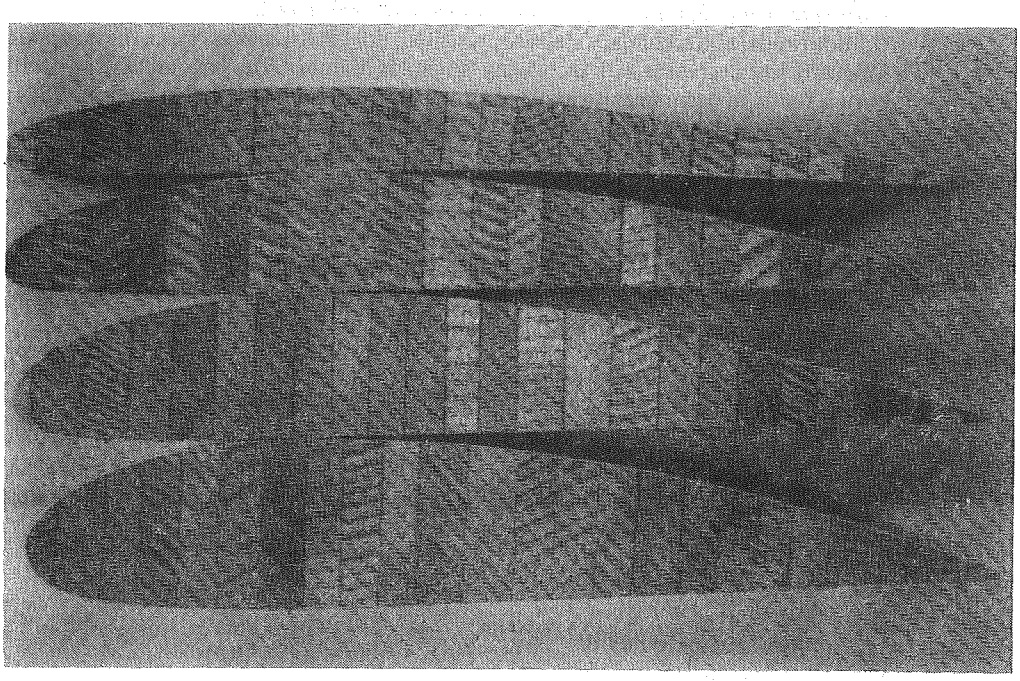

Figure 1 Cross-sectional view, of the NACA 4418, 4415, 4412 and 4409 blades, showing the model construction.

RESULTS AND DISCUSSION

The aerodynamic characteristics are discussed in three sub-sections. Firstly, the effect of variation in Reynolds number is given for infinite aspect ratio blades of different thickness ratios. Secondly, the effect of variation in aspect ratio is studied at a fixed Reynolds number for the different thickness ratios. Lastly, the effect of variation in thickness ratio is presented at a fixed Reynolds number for the different aspect ratios.

Reynolds Number Effect: Figure 2 shows the lift, drag and pitching moment characteristics versus angle of attack, for an infinite aspect ratio blade, of 0.18 thickness ratio, at RNs of 0.25, 0.50, 0.75 and 1.00 million. The pre-stall lift curve slope is constant at 0.09 per degree over the RN angle studied. This may be compared with the value 0.1 per degree given, for RNs of 3 to 9 million, in Reference 3.

For the RN range studied, the RN effect is noticeable only in and around primary and secondary stall. Although initial stall occurs at the same angle of attack ($\alpha = 18°$) for all four RNs, the C_{Lmax} is found to decrease, from 1.50 to 1.39, with increasing RN. A similar decrease was observed for the 15% thick blade and could be attributed to blade bending and twisting, "which affects the circulation around the wing and causes some loss of lift while increasing the drag" (Ref. 1). However, recent investigations (Ref. 4) have also shown a decrease in C_{Lmax} with increase in RN, for RN up to 1 million. Since those studies are for stiff blades, the effect of bending and twisting may not be strong. Rather, this might be a low RN phenomenon. These results are in direct contradiction to what might be expected (Ref. 3) for a "true" 2-D section: an increase in C_{Lmax} with increasing RN. While the present results are for low (up to 1 million) RN, the results of Reference 3 are for a considerably higher (3 to 9 million) RN range.

The work of Loftin and Smith (Ref. 5) is also relevant. They show the C_{Lmax} for an NACA 4415 section decreasing with an increase in RN from 0.7 million to 1 million. However, they show the opposite effect for a NACA 4412 section. The authors are unaware of any comparative data for RN less than 0.7 million. The closest is the compilation (Ref. 6) for model airplane airfoils in the RN angle 60,000 to 250,000. Those C_{Lmax} values, while not reliable because of hysteresis effects, are seen to vary erratically with increasing RN.

The higher RN (0.75 and 1.00 million) lift characteristics are found to cross the lower RN characteristics beyond initial stall. The local minima for the high RN characteristics are of larger magnitude (1.07 versus 0.92) and occur later ($\alpha = 35°$ versus $\alpha = 31°$) than those of the lower RNs. Furthermore, the stall for the higher RNs is gentler. For the RN range studied, secondary stall ($C_L \approx 1.15$) occurs at 42°. Beyond secondary stall, the lift decreases with increasing angle of attack. This 'double-humped' lift curve was seen for the NACA 4415 section and occurs for all the NACA 44XX sections studied here.

The drag rises rapidly and is somewhat RN sensitive beyond C_{Lmax}. As discussed for the 15% thick blade, the maximum drag value (2.06) is roughly the same as that for a flat plate and occures around an angle of attack between 90 and 100 degrees. It will be seen in a later sub-section that this is true for all AR and thickness ratio combinations.

The pitching moment curves are relatively flat in the pre-stall region, except for the lowest RN characteristic which is somewhat erratic. The characteristics have negative slopes in the high angle of attack regions.

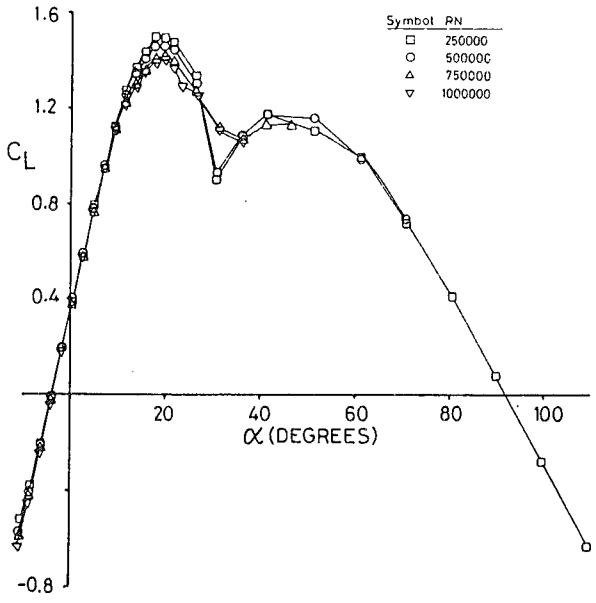

(a) Lift

Figure 2 Aerodynamic Coefficients of the NACA 4418 Airfoil, Infinite Aspect Ratio.

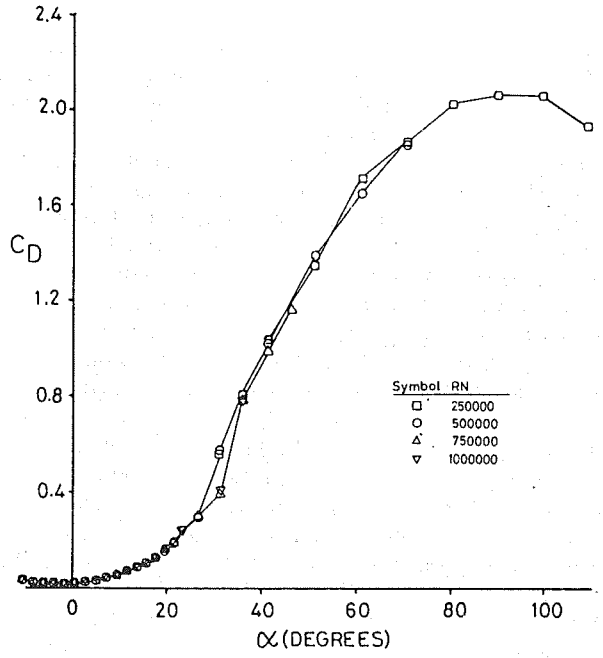

(b) Drag

Figure 2 Continued.

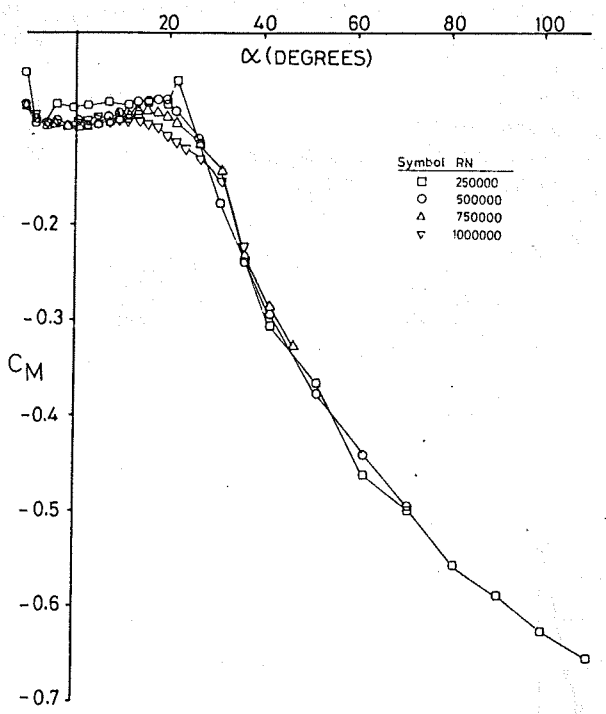

(c) Pitching Moment

Figure 2 - Concluded.

Figure 2 Concluded.

Figure 3 shows results for the 12% thick, two dimensional (AR = ∞) blade. The 'double humped' lift characteristic that was observed for the 18% thick blade, also occurs for the 12% blade. However, the RN effect is less pronounced. C_{Lmax} decreases from 1.35 to 1.32 for a RN increase from 0.25 million to 0.75 million. Stall occurs uniformly at 17.5° angle of attack. The pre-stall lift curve slope is 0.09 per degree as compared to the value of 0.1 given in Ref. 3. The local minimum is the same for all RNs. The magnitude ($C_L \approx$ 0.9) is roughly the same as the values for NACA 4418 and NACA 4415. However, the minima for this thickness ratio occur at a lower angle of attack ($\alpha = 26°$). Secondary stall ($C_L = 1.2$) occurs near 44° and C_{Dmax} (2.06) is near an angle of attack of 90°. The low RN pitching moment curve is somewhat erratic.

For the 9% thick airfoil (Figure 4),the RN effect is not confined to the primary and secondary stall regions. Rather, it is spread over the entire angle of attack range. This could be attributed to the large amount of bending and twisting that the thin blade undergoes. Initial stall occurs at 15° and the local minima (0.92) are at 25°. The drag and pitching moment curves follow the same trends as those mentioned for the 18% and 12% thick blades.

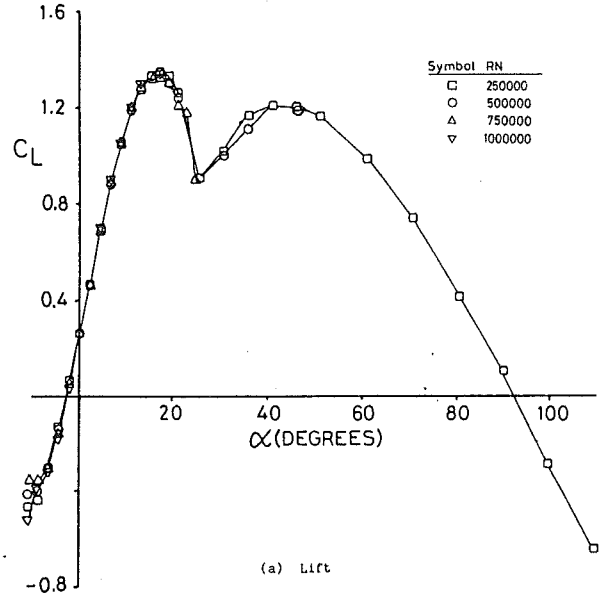

Figure 3 Aerodynamic Coefficients of the NACA 4412 Airfoil, Infinite Aspect Ratio.

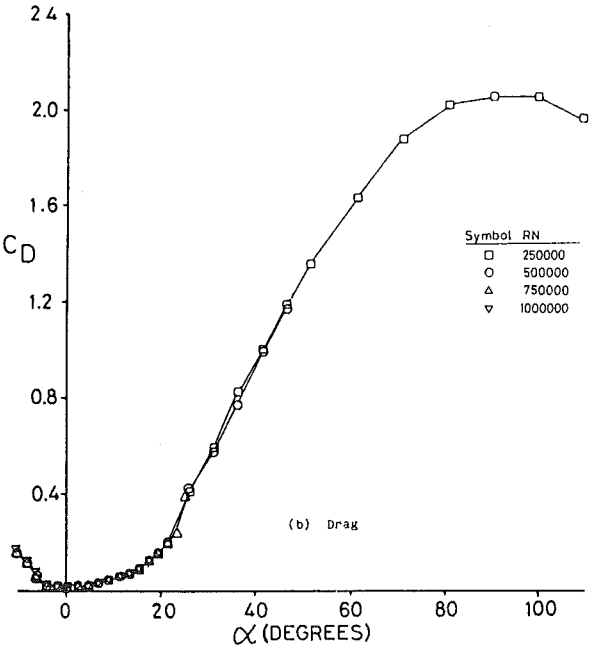

Figure 3 Continued.

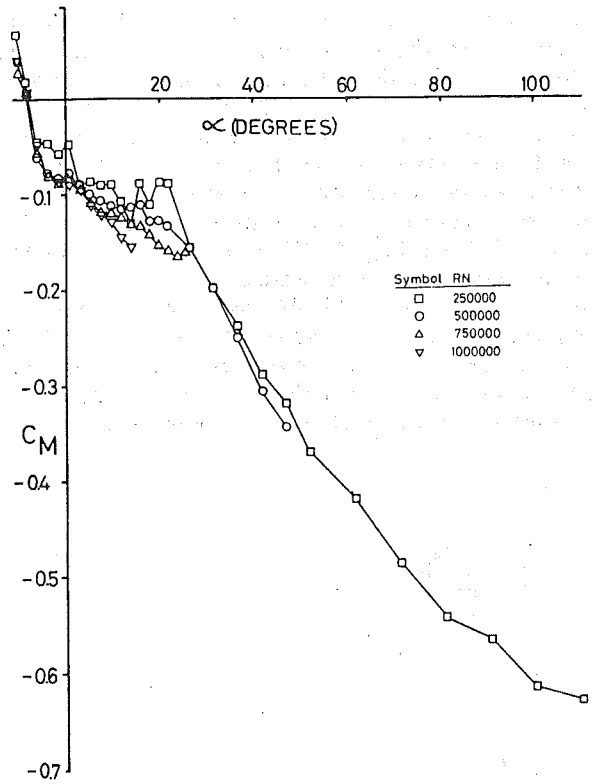

(c) Pitching Moment

Figure 3 Concluded.

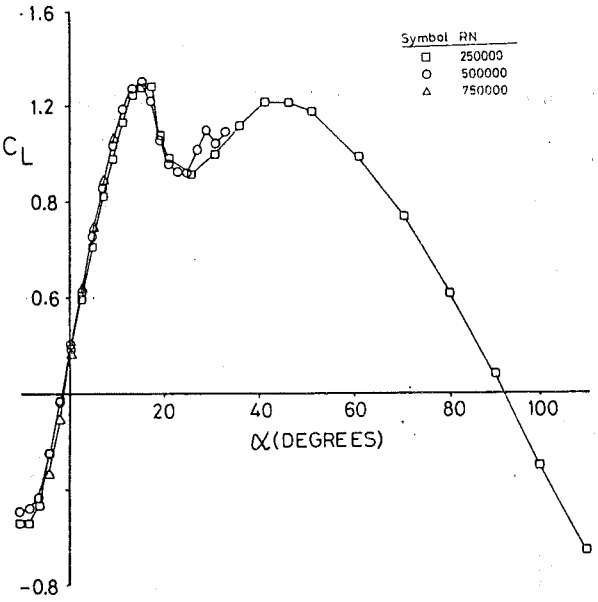

(a) Lift

Figure 4 Aerodynamic coefficients of the NACA 4409 Airfoil, Infinite Aspect Ratio.

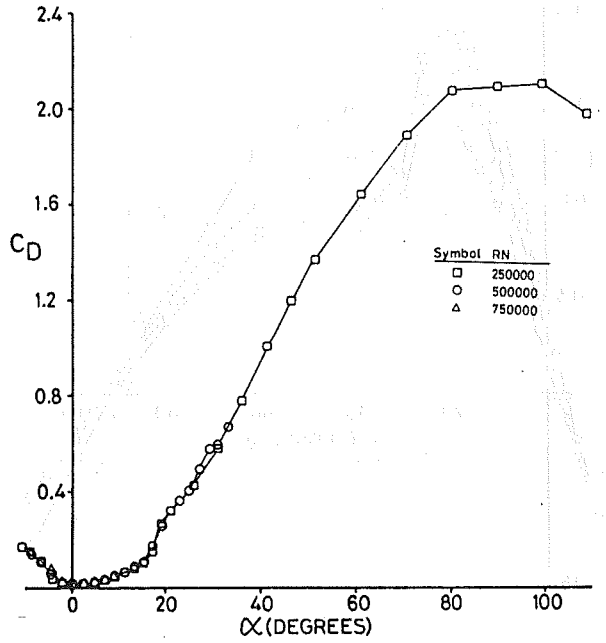

(b) Drag

Figure 4 Continued.

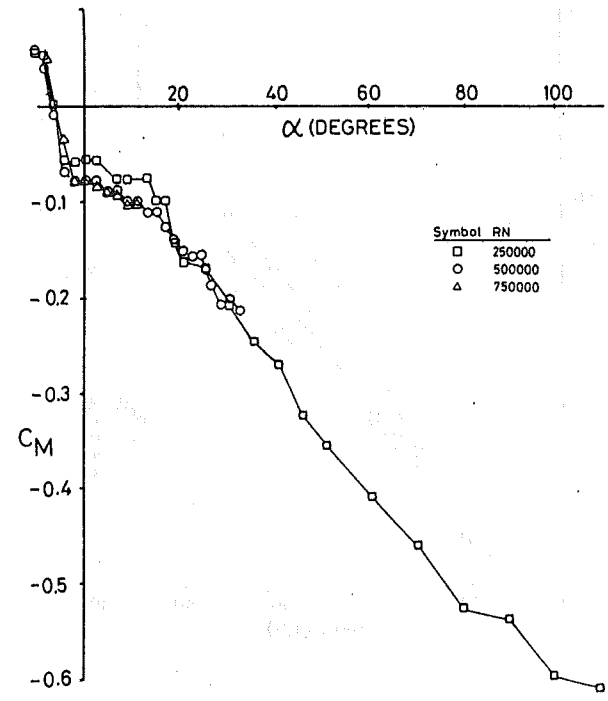

(c) Pitching Moment

Figure 4 Concluded.

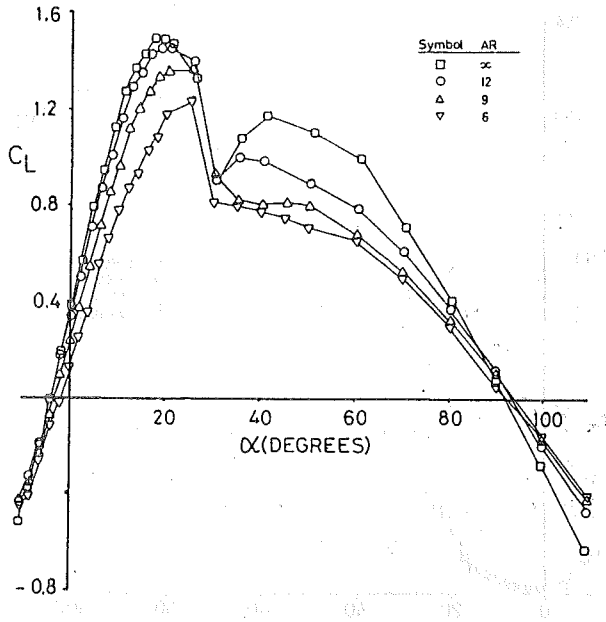

(a) Lift

Figure 5 Effect of Aspect Ratio on the Aerodynamic Coefficients of the NACA 4418 Blade at RN = 0.25×10^6.

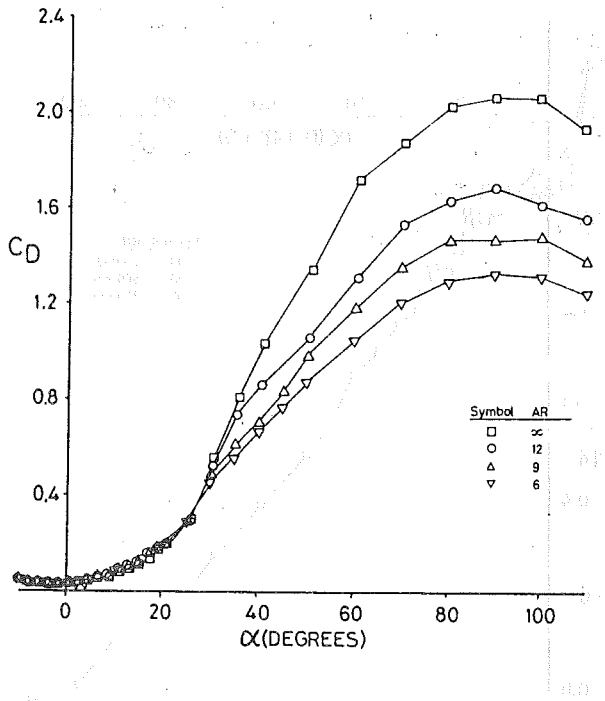

(b) Drag

Figure 5 Concluded.

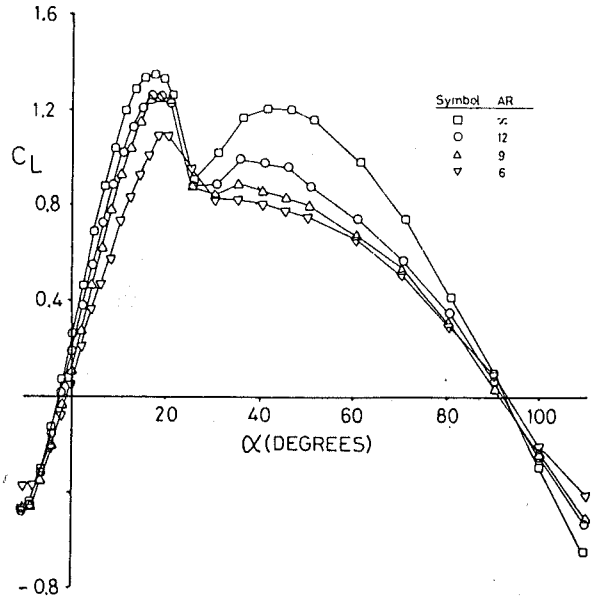

(a) Lift

Figure 6 Effects of Aspect Ratio on the Aerodynamic Coefficients of the NACA 4412 Blade at RN = 0.25×10^6.

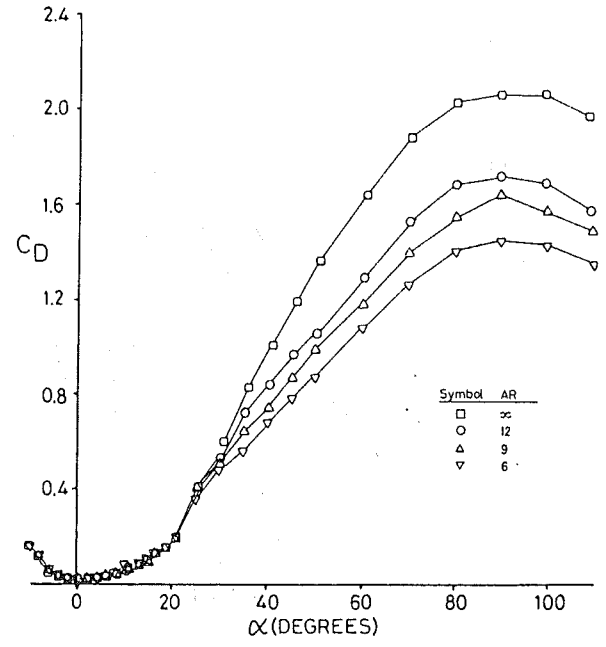

(b) Drag

Figure 6 Concluded.

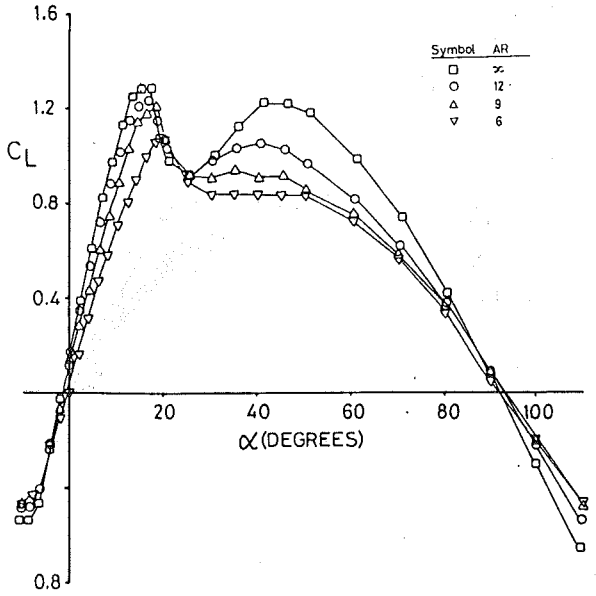

(a) Lift

Figure 7 Effect of Aspect Ratio on the Aerodynamic Coefficients of the NACA 4409 Blade at RN = 0.25×10^6.

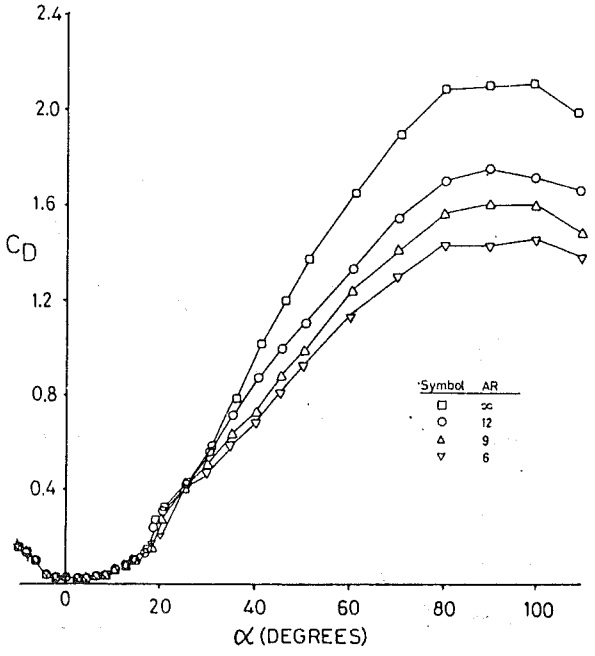

(b) Drag

Figure 7 Concluded.

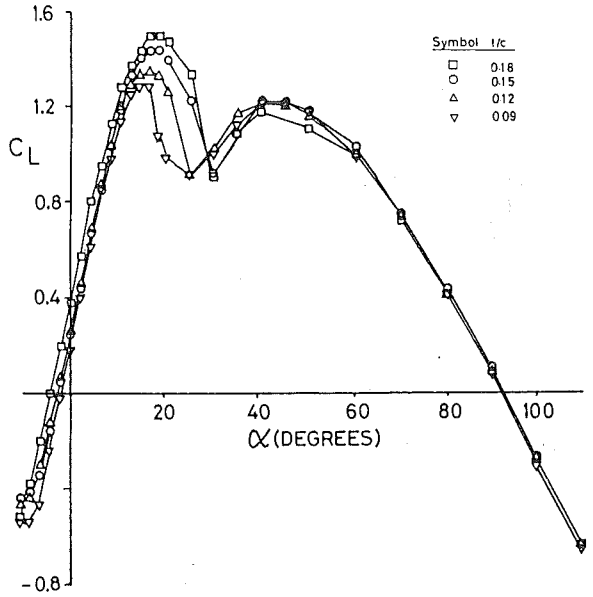

(a) Lift

Figure 8 Effect of Thickness Ratio on the Aerodynamic Coefficients of Blades with NACA 44XX Series sections. RN = 0.25×10^6. Infinite Aspect Ratio.

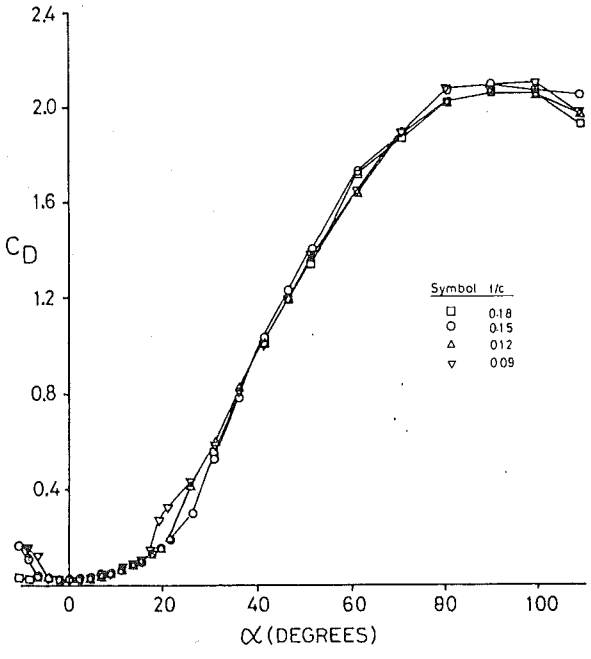

(b) Drag

Figure 8 Concluded.

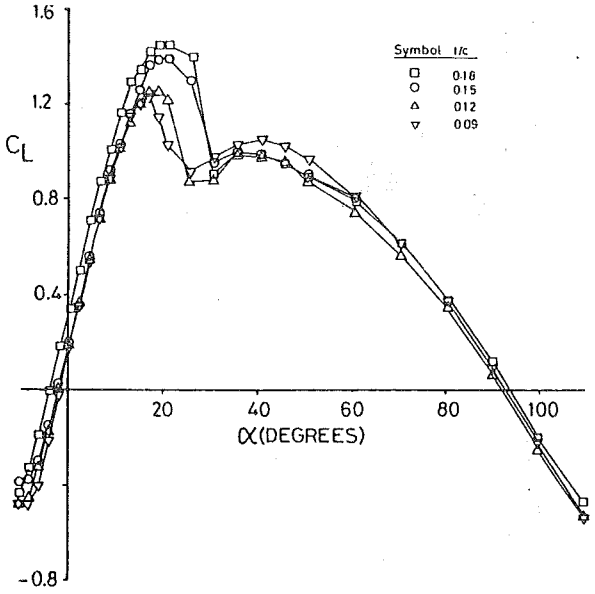

(a) Lift

Figure 9 Effect of Thickness Ratio on the Aerodynamic Coefficients of Blades with NACA 44XX Series Sections. RN = 0.25×10^6. AR = 12.

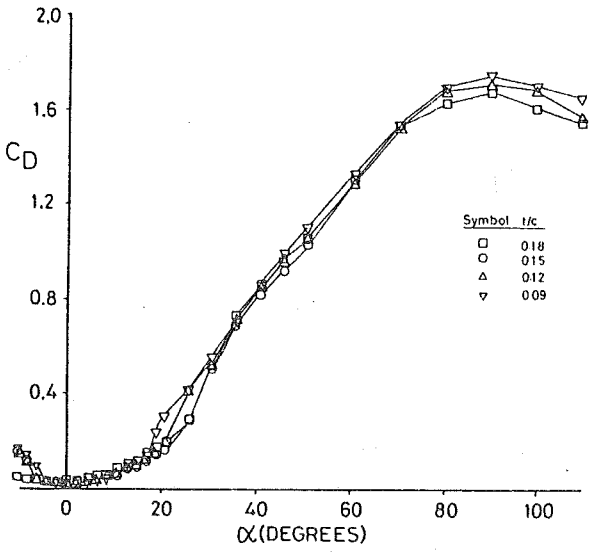

(b) Drag

Figure 9 Concluded.

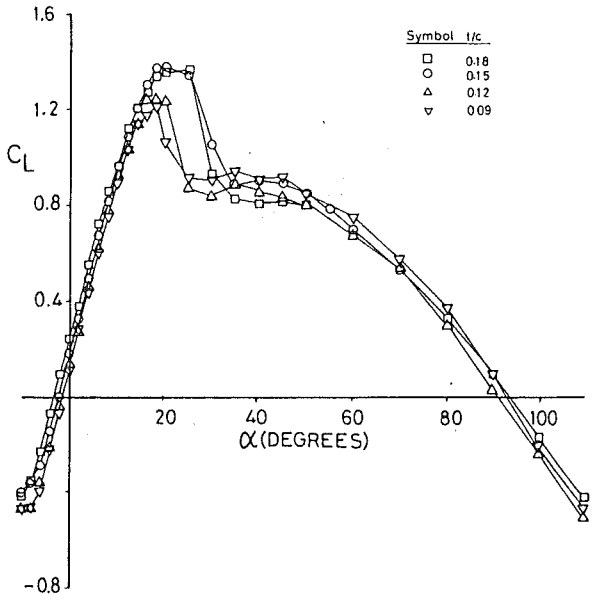

(a) Lift

Figure 10 Effect of Thickness Ratio on the Aerodynamic Coefficients of Blades with NACA 44XX Series Sections. RN = 0.25×10^6. AR = 9.

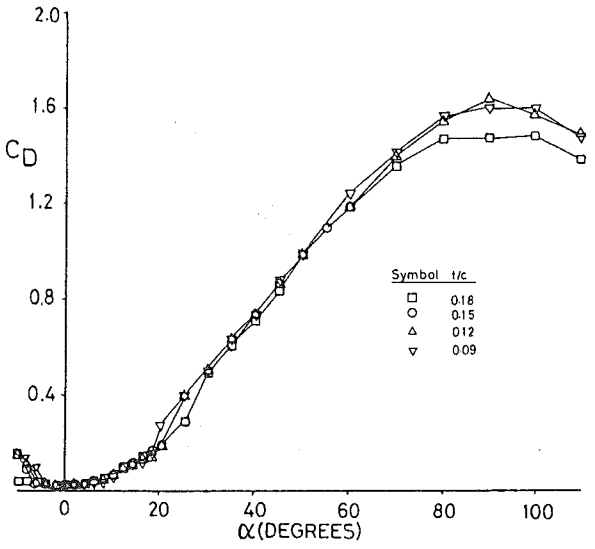

(b) Drag

Figure 10 Concluded.

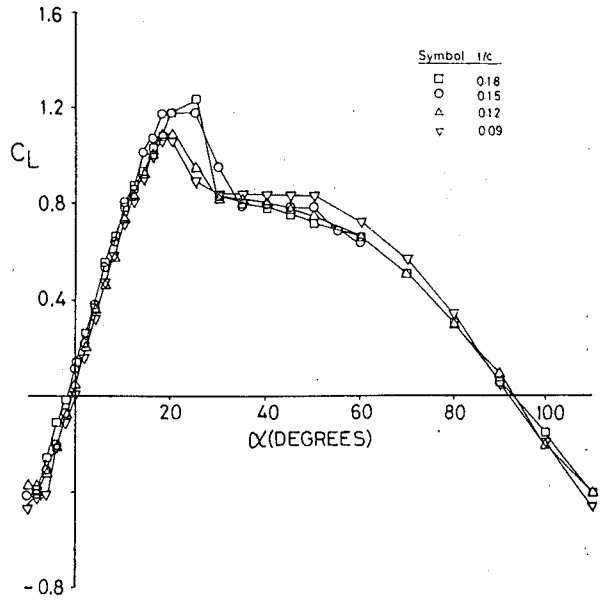

(a) Lift

Figure 11 Effect of Thickness Ratio on the Aerodynamic Coefficients of Blades with NACA 44XX Series Sections. RN = 0.25×10^6. AR = 6.

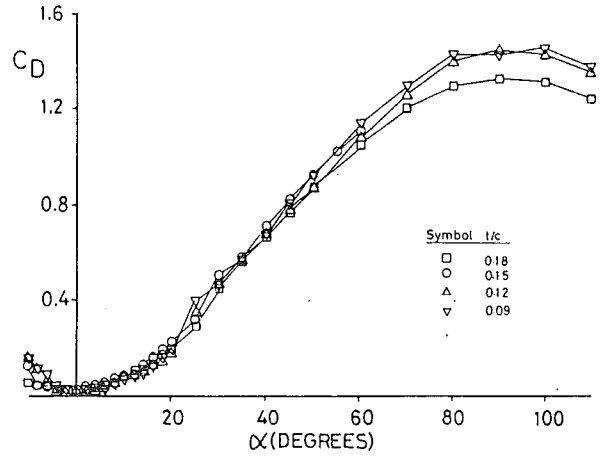

(b) Drag

Figure 11 Concluded.

POST STALL STUDIES

Effect of Aspect Ratio: The aspect ratio effect is presented for each of the three blades (18%, 12% and 9%), in the form of lift and drag characteristics, in Figures 5, 6 and 7. These results are for a RN of 0.25 million. As was previously noted for the 15% thick blade (Ref. 1), a general lowering of the lift curve with decreasing aspect ratio is observed over the angle of attack range $-10°$ to 90°. The C_{Lmax} decreases with decreasing aspect ratio as does the lift curve slope. The stalling angle of attack appears to increase slightly with decreasing aspect ratio. Secondary stall becomes less pronounced as the aspect ratio is decreased. An interesting consequences is that for an AR of 6 there is no second local maximum in the C_L curves of Figures 5, 6 and 7.

The drag is significantly reduced in the post stall region, as the aspect ratio is decreased. For the 18% thick blade, there is a 35% drop in C_{Dmax} (2.06 to 1.33) for an AR decrease from ∞ to 6. For the 9% thick blade, the corresponding reduction in the maximum drag value is 32% (2.10 to 1.43).

Beyond stall, the blade lift and drag characteristics are strongly governed by aspect ratio. By comparison, the post-stall RN effect is not as strong. Smaller aspect ratio results in lower post-stall lift and drag coefficients. This may be attributed to the greater flow leakage around the tip that relieves the pressure differential between the blade upper and lower surfaces.

As stated earlier, the results in this sub-section are for a RN of 0.25 million. The behaviour at higher RN may be inferred from these figures and the RN effect presented above, but is given in detail in Ref. 2.

Effect of Airfoil Thickness: The effect of varying the airfoil thickness is presented for the four thickness ratios, in Figures 8 through 11. These figures are for constant RN (= 0.25 million) with AR of ∞, 12, 9 and 6 respectively.

The airfoil thickness affects C_{Lmax} in that it decreases with decreasing thickness ratio. These results, which are for RNs up to 1 million, seem to contradict Reference 3 where the results are for RNs of 3 to 9 million. However, Reference 5 shows a decrease in C_{Lmax} with thickness ratio for two NACA 44XX airfoils for RN less than 1 million. A crossover in the maximum lift coefficient versus RN curves, for NACA 4415 and NACA 4412, occurs at a RN of 1 million. Beyond one million, C_{Lmax} is found to increase with decreasing thickness ratio.

α_{stall} decreases marginally with decreasing thickness ratio. Primary stall is gentler for the blades with thicker airfoil sections. This may be attributed to the better leading edge suction that arises from a larger nose radius of curvature. The pre-stall lift curve slope, however, is largely unaffected by thickness ratio change. Although the local minimum lift coefficient is the same for all four thicknesses, the angle at which this occurs decreases with decreasing thickness. In general, the post-stall drag coefficient increases with decreasing airfoil thickness.

A change in thickness ratio of a blade does not have as significant an effect, on the post-stall lift and drag characteristics, as does a change in the aspect ratio. The conclusions presented in this section are generally true for the entire RN range studied (Ref. 2).

CONCLUSIONS

Force and moment data are presented for untwisted blades with NACA 44XX series sections with aspect ratios of ∞, 12, 9 and 6 for Reynolds Numbers of 0.25, 0.50 0.75 and 1.00 million. From these data the following conclusions are drawn:

1. For all sections that were studied, both initial and secondary stall are present over the angle of attack range of -10 to 110 degrees. The maximum drag coefficient (2.06 to 2.10) occurs at an angle of attack between 90 and 100 degrees. The pitching moment has a relatively flat characteristic in the pre-stall range and has a negative slope beyond stall.

2. For the thicker blades, the effect of variation in Reynolds Number is noticeable only in and around stall. The maximum lift coefficient decreases with increasing Reynolds Number and the stall is gentler for the higher Reynolds Numbers. The post-stall drag is somewhat Reynolds Number sensitive. For the thinnest blade, the Reynolds Number effect is not confined to the region in and around stall. Rather, it is spread over the entire angle of attack range.

3. The lift and post-stall drag coefficients decrease with increasing aspect ratio and secondary stall becomes less pronounced. The maximum drag coefficient

is reduced by one-third when the aspect ratio is decreased from infinity to 6.

4. The lift coefficient and stalling angle of attack both decrease with decreasing airfoil thickness ratio, while the post-stall drag coefficient increases. The thicker blades have a gentler stall and this is attributed to better leading edge suction. The pre-stall lift curve slope is unaffected by thickness ratio. These thickness ratio effects are true for all aspect ratios.

5. The results show that the post-stall aerodynamic characteristics are strongly affected by changes in aspect ratio, while the thickness ratio and Reynolds Number effects are relatively weak. The aspect ratio effect is attributed to the increasing tip-flow leakage that occurs for decreasing aspect ratios.

REFERENCES

1. Ostowari, C. and Naik, D. *Post Stall Studies of Untwisted Varying aspect Ratio Blades with a NACA 4415 Airfoil Section – Part 1, Wind Engineerimg, Vol.8 No.3, 1984.*

2. Ostowari, and Naik, D. *Post-Stall Wind Tunnel Data for NACA 44XX Series Airfoil Sections, a Subcontract Report, SERI/STR-217-2559, Solar Energy Research Institute, Golden, Colorado, January 1985.*

3. Abbott, I.H. and Von Doenhoff, A.E. *Theory of Wing Sections, Dover Publications, Inc., New York, 1959.*

4. Wentz, Jr., W.H. *Wichita State University, Wichita, Kansas. Private communication, of unpublished data, with authors.*

5. Loftin, Jr., L.K. and Smith..H.A. *Aerodynamic Characteristics of 15 NACA Airfoil Sections at Seven Reynolds Numbers.*

6. Althaus, D. *Profilpolaren für den Modellflug, Windkanalmessungen an Profilen im kritischen Reynoldszahlbereich, Neckar-Verlag, Vs-Villingen, 1980*